Biochemical and Biophysical Research Communications 463 (2015) 154–160

Contents lists available at ScienceDirect

Biochemical and Biophysical Research Communications

journal homepage: www.elsevier.com/locate/ybbrc

Mutational analysis of *Mycobacterium tuberculosis* lysine ε-aminotransferase and inhibitor co-crystal structures, reveals distinct binding modes

Sarvind Mani Tripathi [1], Aparna Agarwal [1], Ravishankar Ramachandran*

Molecular & Structural Biology Division, Central Drug Research Institute, Sector 10, Jankipuram Extension, Sitapur Road, Lucknow 226031, U.P., India

ARTICLE INFO

Article history:
Received 16 April 2015
Available online 20 May 2015

Keywords:
Lysine ε-aminotransferase
Crystal structure
Glu243 switch
2-Aminomethyl piperidine derivative
α-ketoglutarate
Mycobacterium tuberculosis

ABSTRACT

Lysine ε-aminotransferase (LAT) converts lysine to α-aminoadipate-δ-semialdehyde in a PLP-mediated reaction. We mutated active-site T330, N328 and E243, and structurally rationalized their properties. T330A and T330S mutants cannot bind PLP and are inactive. N328A although inactive, binds to PLP. E243A retains activity, but binds α-ketoglutarate in a different conformation. We had earlier identified 2-aminomethyl piperidine derivative as a LAT inhibitor. The co-crystal structure reveals that it mimics binding of C5 substrates and exhibits two binding modes. E243, that shields R422 in the *apo* enzyme, exhibits conformational changes to permit the binding of the inhibitor in one of the binding modes. Structure-based analysis of bound water in the active site suggests optimization strategies for synthesis of improved inhibitors.

1. Introduction

Lysine ε-aminotransferase (LAT; EC 2.6.1.36) is a pyridoxal 5′-phosphate (PLP)-dependent enzyme involved in lysine metabolism in a range of organisms and converts lysine to α-aminoadipate δ-semialdehyde. It's action represents the first step of β-lactam antibiotic synthesis in actinomycetes [1,2]. Overall, it catalyzes a reaction involving the transfer of the ε-amino group of L-lysine to α-ketoglutarate to yield L-glutamate and α-aminoadipate-δ-semialdehyde. The latter is subsequently dehydrated and forms piperidine 6-carboxylate [3]. In the reverse reaction, the chemical changes occur to the α-amino group of glutamate substrate.

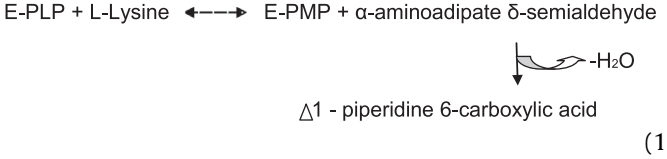

(1)

(2)

We had earlier presented direct evidence of a Glu243 'switch' in LAT that allows for this and also suggested that this is conserved in a subgroup of aminotransferases [4,5].

Lysine ε-aminotransferase from *Mycobacterium tuberculosis* (MtLAT) belongs to subgroup II of the fold type-I aminotransferases and is highly upregulated (~40 folds) in nutrient starved tuberculosis models designed to mimic latency/persistence. Other archetypal members of fold type-I aminotransferases, of which LAT is a member, includes ornithine aminotransferase and γ-amino butyrate aminotransferase respectively [6–8]. In several analyses, LAT has been ranked as a potential potent anti-tuberculosis target [9,10]. Intriguingly; all components of the β-lactam antibiotic synthesis pathway have not been identified in mycobacteria despite the full-genome sequence being available. This raises the possibility that the enzyme might have adapted to perform other functions in *M. tuberculosis*.

M. tuberculosis LAT exists as a dimer where the active site is made up of residues from both subunits. Our earlier crystal structures of LAT identified that T330 and N328 from the symmetry-related subunit interact with PLP and Lys substrate respectively. We also found that the E243 binds to R422 in the presence of Lys substrate while it switches away to permit the binding of C5 substrates like Glu in the second half of the reaction. We therefore

Abbreviations used: LAT, lysine ε-aminotransferase; MtLAT, *Mycobacterium tuberculosis* LAT; PLP, pyridoxal5′-phosphate; PMP, pyridoxamine 5′-phosphate.

* Corresponding author. Fax: +91 522 2772490.
E-mail address: r_ravishankar@cdri.res.in (R. Ramachandran).

[1] These authors contributed equally to the manuscript.

http://dx.doi.org/10.1016/j.bbrc.2015.05.055
0006-291X/

mutated these conserved residues to probe their roles in the enzyme's activity and also solved the crystal structures of the mutants. We found that mutations to T330 and N328 resulted in inactive enzyme for different reasons respectively. On the other hand, E243A mutant retained activity, albeit with differences, and binds to the C5 substrate α-ketoglutarate (KGA) in a different conformation. We had earlier identified a 2-aminomethyl piperidine derivative as an inhibitor of the LAT enzyme through virtual screening experiments [11]. The presently reported co-crystal structure shows details of the interaction of this inhibitor with the enzyme and suggests that the inhibitor mimics the binding of C5 substrates. Analysis of conserved water molecules in the active site suggests a strategy for optimization of the potency of this inhibitor.

2. Materials and methods

2.1. Site-directed mutagenesis

E. coli strain DH5α was used for cloning while the XL1Blue strain was used for site directed mutagenesis.

All four mutants *viz*. T330A-MtLAT, T330S-MtLAT, E243A-MtLAT, and N328A-MtLAT were generated by sense-antisense primer method and the *pET23a-MtLAT* template using the following primer pairs. Sense and antisense primers for T330A (sense: 5′-CGGCTCAACTCGGCATGGGGTGGCAAT-3′, antisense: 5′ -ATTGC-CACCCCATGCCGAGTTGACCCG-3′), E243A (sense: 5′-GCAGAACCAA TCCAGGGCGCAGGTGGC-3′, antisense: 5′-GTCACCACCTGCGCCCTG-GATAGGTTC-3′) and N328A (sense: 5′-CCATCACGGCTTGCCTCGA-CATGGGGT-3′, antisense: 5′ACCCCATGTCGAGGCGACCGGTGA3′ respectively). The presence of respective mutations was confirmed by sequencing.

2.2. Expression and purification of MtLAT and mutants

Escherichia coli C41 (DE3) was used for over-expression of pET23a MtLAT and its variants [4]. The purification of respective mutant enzymes was carried out same as reported earlier for the native enzyme [4].

2.3. Enzyme assays

Enzymatic activities of native as well as of mutants were determined by detecting Δ^1-piperidine-6-carboxylate respectively [5,12]. The amount of Δ^1-piperidine-6-carboxylate formed was calculated by using extinction coefficient of 2800 L mol^{-1} cm^{-1} [12]. Michaelis constants for L-lysine and α-ketoglutarate substrates were determined either by varying concentrations of L-lysine from 0.5 mM to 10 mM at several concentrations of α-ketoglutarate or by varying concentrations of α-ketoglutarate from 0.5 mM to 10 mM at several concentrations of L-lysine. The initial data were plotted as 1/V (micrograms of Δ^1-piperidine-6-carboxylate formed per milliliter per hour) versus 1/[S] (millimoles of substrate). Kinetic parameters were calculated by fitting the values calculated from secondary plots ($1/V_{max}$) versus inverse of substrate concentration (1/[S]) to the Lineweaver-Burke equation (1)/$V_o = (K_m/V_{max}$ X [S]) + $1/V_{max}$ using *GraphPad Prism* software.

2.4. Estimation of PLP content

Purified MtLAT and its mutants were dialyzed extensively against 50 mM Tris (7.2), 50 mM NaCl, 5 mM EDTA and 2 mM βMe. The dialyzed enzyme samples (1.2 mg/ml) were incubated separately with 0.1 M NaOH for 5 min and the absorbance was measured at 388 nm. The PLP content was determined, taking the molar absorption coefficient of PLP in 0.1 M NaOH as 6600 M^{-1} cm^{-1} at 388 nm [13].

2.5. UV–vis spectroscopy

Absorption spectra of native and mutant enzymes were recorded at 25 °C on a Perkin Elmer double beam spectrophotometer in 20 mM phosphate buffer (pH 7.2) and 50 mM NaCl at protein concentration of 15 μM.

2.6. Circular dichroism spectroscopy

CD measurements were made using a Jasco J810 spectropolarimeter calibrated with ammonium (+)-10-camphorsulfonate. CD spectra were obtained at enzyme concentrations of 2 and 10 μM for far-UV CD and visible CD measurements, respectively, with a 2-mm cell at 25 °C. Visible CD spectra were

Table 1
Data collection and refinement statistics.

	T330S	E243A	N328A	INH (B)
Data collection				
Cell dimensions				
a, *b*, *c* (Å)	103.2,103.2, 98.1	102.8,102.8, 97.8	103.4,103.4, 98.1	102.8,102.8, 97.8
Resolution (Å)	2.2 (21.5)[a]	2.7 (21.4)	1.95 (21.5)	2.5 (20.4)
R_{sym} or R_{merge}	0.10 (0.40)	0.14 (0.43)	0.06 (0.50)	0.14 (0.50)
$I/(\sigma)I$	13.3(4.1)	8.3(3.0)	8.3(3.0)	10.5(3.2)
Completeness (%)	97.4 (99.3)	99.6 (100)	99.9 (100)	92.2 (95.3)
Redundancy	5.5 (5.3)	3.5 (3.5)	5.0 (4.9)	5.0 (4.8)
Refinement				
R_{work}/R_{free}	15.87/18.07	15.10/19.42	16.60/18.50	16.10/20.50
No. atoms				
Protein	3350	3350	3350	3350
Ligand/ion	15	25	15	35
Water	186	186	217	108
B-factors				
Protein	21.98	19.68	25.02	20.97
Ligand/ion	15.70	12.30	22.90	37.90
Water	23.93	20.48	28.20	22.49
r.m.s deviations				
Bond lengths (Å)	0.009	0.012	0.008	0.010
Bond angles (°)	1.216	1.45	1.13	1.408

T330S, E243A, N328A and INH (B) refer to the active-site mutants and inhibitor bound crystal structures respectively.
[a] Highest resolution shell statistics are in parenthesis.

recorded from 500 to 300 nm using 10 μM protein concentrations. The values obtained were normalized by subtracting the baseline recorded for the same buffer under similar conditions.

2.7. Crystallization and data collection

Crystallization of T330S, N328A and E243A and WT-MtLAT with inhibitor, was carried out using protocols described earlier [4]. For crystallization of the T330S-MtLAT mutant, the enzyme was incubated with PLP for 24 h prior to crystallization. Crystals of MtLAT with inhibitor were obtained by incubating the protein solution with 10 mM inhibitor for 24 h before crystallization.

Diffraction data for T330S-LAT, E243A and MtLAT inhibitor complex were collected using a Rigaku RU300 X-ray generator coupled to a MAR345 image plate detector. The data were collected at room temperature from a single crystal mounted in a glass capillary. Data for the N328A mutant was collected from a capillary mounted crystal. Crystals remained stable at room temperature throughout the data collection. MOSFLM [14] and SCALA [15] from the CCP4 suite [16] were used for data processing and scaling respectively. Crystals of all three mutants belong to $P3_121$ space group with one monomer in the asymmetric unit as was the case with the native enzyme. Details of cell dimension, data collection statistics and refinement statistics for these crystals are shown in Table 1.

2.8. Structure determination and model building

The MtLAT structure in its internal aldimine form (PDB code 2CIN) was used as the initial model [4]. Rigid body refinement using Refmac5 was initially carried out. *2Fo-Fc* and *Fo-Fc* maps were calculated and visualized using TURBO-FRODO [17] and COOT [18] respectively. The maps were readily interpretable and electron density of PLP which was omitted from the initial model was clearly visible. MtLAT with inhibitor structure was examined by inspecting the composite omit map and clearly identified electron density corresponding to the inhibitor at the active site. The co-ordinates and the structure factors have been deposited in the Protein Data Bank (http://www.rcsb.org) with accession numbers 2JJG, 2JJF, 2JJE and 2JJH respectively.

3. Results

3.1. Properties of the MtLAT mutants

MtLAT and mutant proteins, T330A, T330S, N328A and E243A were overexpressed in *E. coli* C41 (DE3). The purified proteins respectively ran as a single band on SDS/PAGE at 50 kDa indicating homogeneity. Size-exclusion chromatography analysis using a calibrated Superdex 200 10/300 GL column support that the mutants exist as dimers in solution similar to wild-type MtLAT. The mutations therefore do not disrupt the oligomeric association. UV–VIS spectra of wild-type MtLAT had a major absorbance peak at 420 nm mainly, due to protonated aldimine form and a minor peak at 330 nm Fig. 1A. For N328A, an almost similar spectrum was found. However all E243A preparations showed very weak absorption at 330 nm compared to that found in wild-type and N328A suggesting that this mutant was mainly in the aldimine form when isolated. Near-UV CD spectrum and UV–VIS absorbance experiments clearly showed that T330A and T330S mutants which were

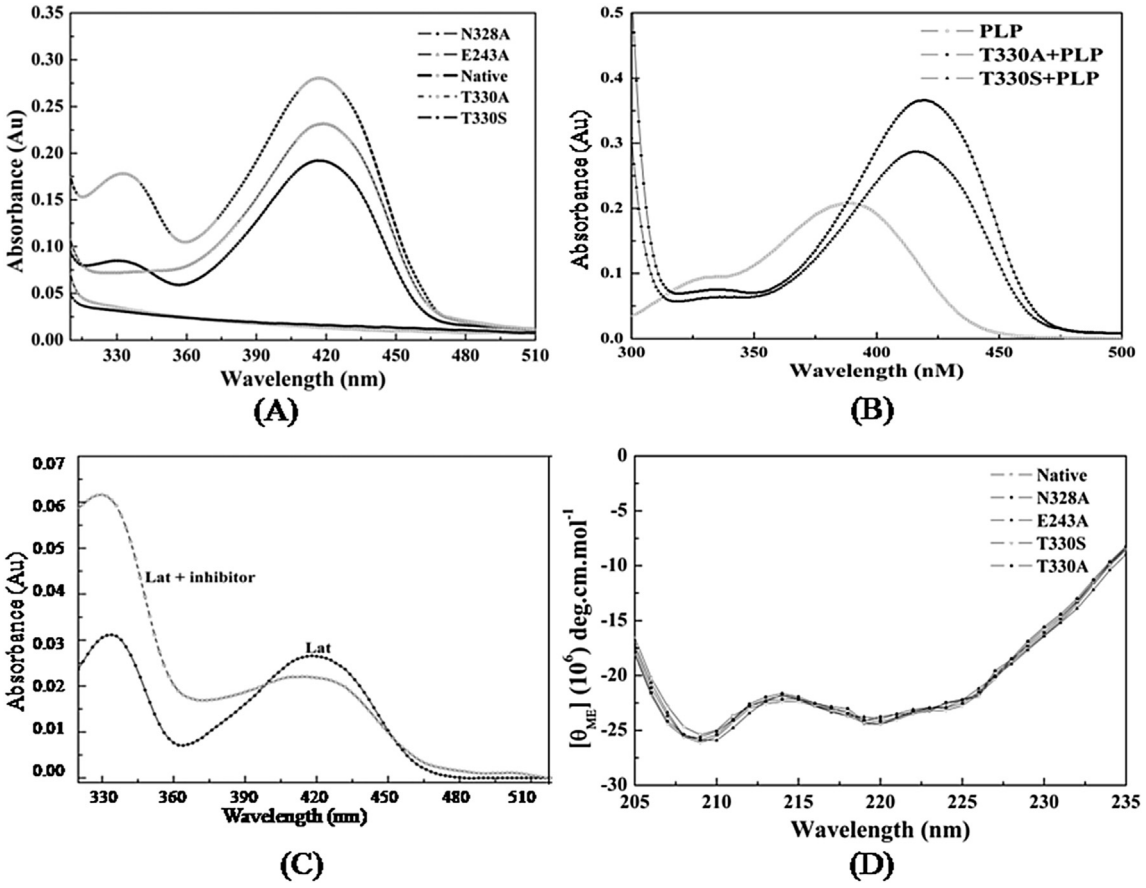

Fig. 1. Spectrophotometric characterization of native and mutant enzymes. (A) UV–VIS spectra of recombinant proteins at 25 °C under standard condition in which they purified. The spectra for individual proteins are marked and labeled distinctly in the figure. (B) UV–VIS spectra of T330A and T330S after incubation with PLP. (C) Absorption spectra of MtLAT after and before incubation with inhibitor. (D) Far-UV CD spectra of MtLAT and its mutants.

Table 2
Kinetic parameters of MtLAT and its mutants.

	MtLAT	E243A	N328A	T330A	T330S
K_m(L-lysine)	1.2 mM	1.7 mM	ND	IA	IA
K_m(KGA)	2.3 mM	1.6 mM	ND	IA	IA
K_{cat}(L-lysine)	55 min^{-1}	70 min^{-1}	ND	IA	IA
K_{cat}(KGA)	86 min^{-1}	60 min^{-1}	ND	IA	IA
PLP/mol	1.0 + 0.1	1.0 + 0.1	1.0 + 0.2	0.0	0.0

ND refers to 'not determinable' due to negligible activity, while IA stands for 'inactive'.

colorless after purification did not contain the co-factor in any form Fig. 1A. The amount of PLP bound to the enzyme was determined for the proteins using a molar absorption coefficient value for PLP 6600 M^{-1} at 388 nm. Analysis of PLP content showed that MtLAT, E243A and N328A contain 1 molecule of PLP/enzyme monomer, while T330A and T330S mutants do not contain PLP. Incubation of T330A and T330S with PLP for 30 min respectively at 4 °C reconstituted the respective mutants to the internal aldimine form and these then show strong peaks at 420 nm Fig. 1B. The far-UV CD spectra of MtLAT and the mutants overlap with each other indicating that the mutations did not result in changes to the secondary structure Fig. 1D. T330A and T330S were totally inactive because these mutants do not contain PLP. On the other hand, N328A shows substantially less activity compared to the native enzyme pointing to its importance in the catalytic cycle Table 2. E243A exhibited activity but with differences as seen above.

3.2. Crystal structures of the mutant enzymes

The crystal structures of the T330S, E243A and N328A mutants were refined to 2.2, 2.7 and 1.95 Å respectively. The electron density maps were of good quality Fig. 2A. T330S, N328A and E243A exhibit r.m.sd. of 0.07 Å, 0.08 Å and 0.1 Å, respectively compared to wild-type enzyme indicating that the overall structure is similar. This is in line with Far-UV CD experiments also. The first 15 residues and the C-terminal hexa-histidine tag were disordered in the electron density maps. The most favored and additionally allowed regions of the Ramachandran plot contained 99.2% of non-proline and glycine residues respectively in the three mutant structures [8]. The asymmetric unit contains a monomer while the dimeric counterpart is generated through crystallographic symmetry. The relative positions of the two domains in a subunit and the inter-subunit interactions in the dimer are affected by the mutations. The pyridine ring and the phosphate of the cofactor are in very similar position in the structures. Further, K300 of the active site forms a Schiff base with PLP in the E243A mutant. Interestingly, density for α-ketoglutarate (KGA) was observed in this structure. A comparison with the native enzyme's complex with KGA showed differences in the conformation of KGA and its interactions in the E243A mutant Fig. 2.

3.3. Co-crystal structure of MtLAT-inhibitor

The crystals of the 2-aminomethyl piperidine derivative inhibitor complex diffract to 2.5 Å. The electron density maps clearly indicated two conformations for the inhibitor Fig. 3A. Modeling of the inhibitor revealed that the piperidine moiety of the inhibitor adopts two different conformations. Correspondingly the side chain of Glu243 adopts two different orientations analogous to those seen in the earlier native MtLAT-KGA complex [4]. The side chain of Glu243 and the pyridine moiety of the inhibitor were refined with partial occupancy of 0.5 in each conformation. The overall structure of the inhibitor complex is largely similar to that of the wild type enzyme except for the described conformational changes. PLP is attached to the protein through a Schiff base linkage with NZ of Lys300. The N2 of the inhibitor is held in place by interactions involving NE and NH2 of Arg170 Table 3. The phenacyl group displaces a couple of conserved water molecules that were seen in the internal aldimine form, and other LAT structures. Other interactions include those with the PLP itself, Asn328, and Glu243 respectively Fig. 3B.

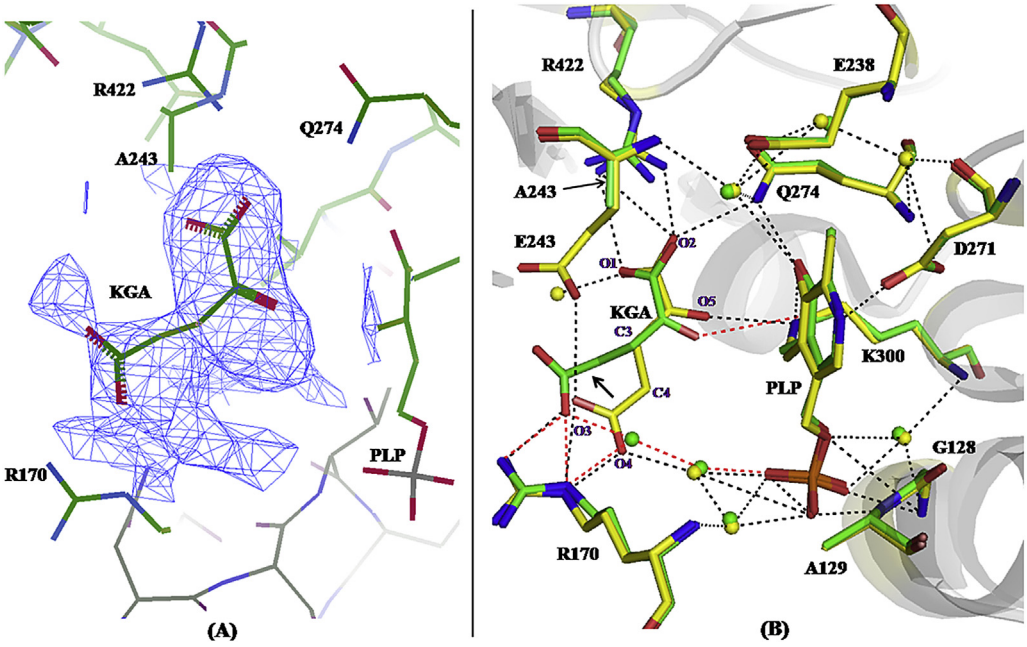

Fig. 2. (A) 2Fo-Fc electron density map of E243A mutant contoured at 1.4 σ around α-ketoglutarate (KGA). The boundKGA moiety exhibits changes in conformation compared to its complex with the native enzyme. Selected residues are also labeled for clarity. (B) Structural superimposition of the MtLAT-KGA complex (*Yellow*) with the E243A-KGA complex (*Green*). Conformational changes in KGA are indicated. (For interpretation of the references to color in this figure legend, the reader is referred to the web version of this article.)

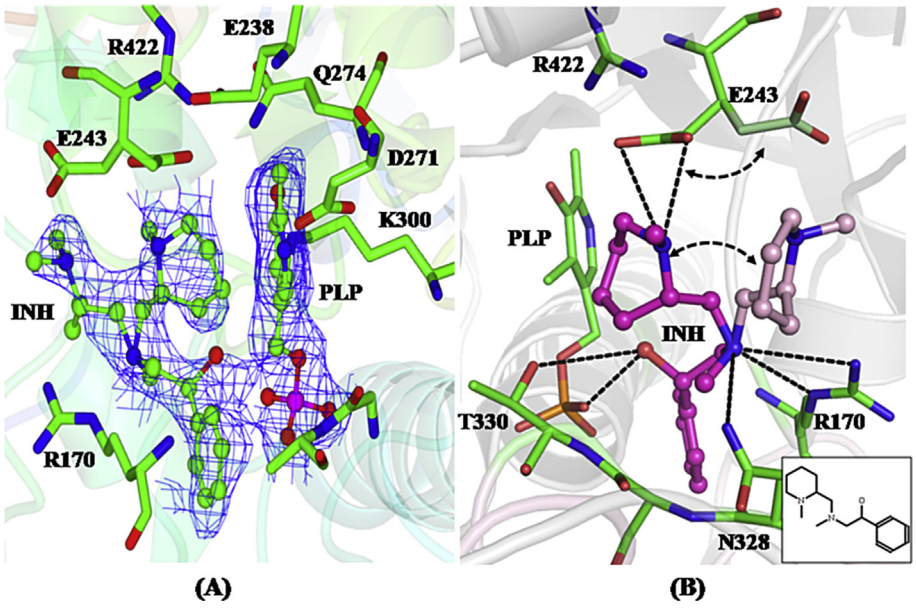

Fig. 3. (A) 2Fo-Fc electron density map contoured around the Inhibitor in its complex with MtLAT. The inhibitor and PLP are shown in ball-and-stick representation and also selected residues are labeled. (B) Interactions of the Inhibitor with MtLAT. The inset shows the 2D representation of the 2-aminomethyl piperidine derivative for clarity. Selected residues are also labeled.

3.4. Active site water clusters

Structurally conserved water molecules in the active site have been exploited to increase the inhibitory potency of designed compounds. Often a polar atom like oxygen or nitrogen of the inhibitor/ligand can take the place of the displaced water oxygen and replace its interactions with the protein through direct or water-mediated interactions [19]. This reportedly contributes up to 20-fold increase in affinity. Using this strategy, the inhibitor's specificity can be enhanced by substituting polar atoms at appropriate locations in it to form hydrogen bonds with structural water in the binding site [20], or by displacing them from the binding site. We therefore analyzed crystallographically identified waters in the PLP and substrate binding site from available MtLAT structures [4]. We superposed the dimer from the eight available MtLAT structures *viz.* 2CIN (internal aldimine form), 2CJH (KGA bound), 2CJD (L-Lysine bound), 2CJG (PMP bound) and the present structures of the mutants (PDB ids 2JJE, 2JJH and 2JJF) onto the MtLAT-inhibitor complex (2JJG). Table 4 summarizes the analysis, while Fig. 4 is a graphic representation of the active site water network. A total of 12 water clusters were observed after superposition of the structures. W1 to W8 are present in almost all MtLAT structures Table 4. W1 to W3 form a network and mediate interactions of PLP with the protein. W4 toW8, located below the PLP moiety in Fig. 4 form another water-network. W4 mediates interactions of PLP with the substrate while W5 apparently helps and mediates interactions of the co-factor with R170. W9 does not directly interact with either PLP or the substrate. W10 only interacts with KGA in the structure of its complex (PDB: 2CJH) while W11 interacts with the Lysine substrate (PDB: 2CJD). Interestingly, W12 that is present in the E243A mutant structure has a spatial disposition similar to that of an oxygen atom of KGA in its complex with native MtLAT. Additionally, the analysis highlights that binding of the inhibitor displaces highly conserved water molecules W4 and W5 respectively.

Table 3
Interactions of inhibitor (INH) and α-ketoglutarate (KGA) with respective proteins. Distances are in Å units.

(A)		
INH	**MtLAT protein**	**Distance**
O	PLP-P	3.5
	PLP-OP2	2.5
	PLP-OP4	3.5
N2	Arg170-NH2	3.5
	Arg170-NE	3.0
	Asn328*-ND2	3.3
N1	Glu243-OE1	3.4
	Glu243-OE2	3.1
(B)		
KGA	**E243A protein**	**Distance**
O3	Arg170-NH2	2.6
	Asn328*-ND2	3.3
	Arg170-NE	2.6
O1	Arg422-NH2	3.2
O2	Arg422-NH2	2.7
	Gln274-NE2	3.1

Table 4
Water cluster analysis, occupancy of water molecules in the active site of MtLAT.

	2CIN	2CJH	2CJG	2CJD	2JJH	2JJE	2JJF	2JJG
W1	+	+	+	+	+	+	+	+
W2	+	+	+	+	+	+	+	+
W3	+	+	+	+	+	+	+	+
W4	+	+	+	+	+	+	+	NP
W5	+	+	+	+	+	+	+	NP
W6	+	+	+	+	−	+	+	+
W7	+	+	+	+	−	+	+	+
W8	+	+	+	+	+	+	+	+
W9	+	−	−	−	−	+	+	+
W10	−	+	−	−	−	−	−	−
W11	−	−	−	+	−	−	−	−
W12	−	−	−	−	+	−	−	−

"+" refers to the occurrence of a particular water while "−" refers to its absence; "NP refers to those cases where the occurrence of a water molecule is not possible because of the binding of substrate or inhibitor.

4. Discussion

Lysine-ε-aminotransferase belongs to a subfamily of aminotransferases that very elegantly, through a Glu243 (in MtLAT)

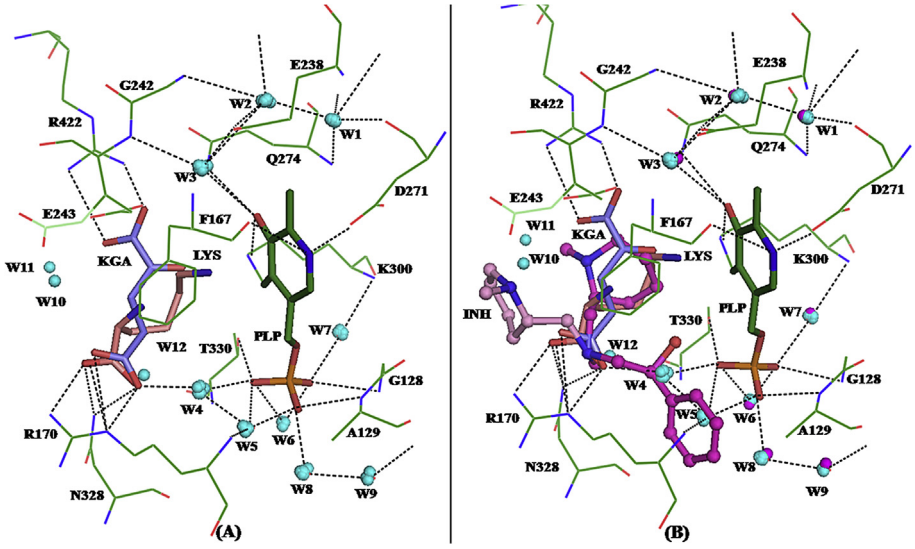

Fig. 4. Conserved water clusters in the active site of MtLAT. (A) Water molecules from all superposed MtLAT structures are represented as blue spheres (*see also* Table 4). KGA and PLP moieties are also depicted and labeled. (B) The MtLAT inhibitor superposed with water clusters. The phenacyl group of the inhibitor displaces the water W4 and W5. *Magenta* colored molecules are from the inhibitor complex, while *cyan* colored spheres indicate water molecules conserved in the other LAT structures. (For interpretation of the references to color in this figure legend, the reader is referred to the web version of this article.)

'switch', solve the problem of distinguishing between similar substrates and carrying out specific reactions on them [4]. MtLAT is an intriguing member of the family; although it is highly upregulated under non-replicative conditions in *M. tuberculosis*, its role is not clearly understood. All members of the lysine metabolism pathways have not yet been identified in mycobacteria despite the sequence being available [10,21]. It has been consistently flagged as an important potential target in different analyses based on its up-regulation under nutrient starvation and other studies involving *M. tuberculosis* [22].

We found that T330 and N328 from the symmetry-related subunit that form a part of the active site, are conserved in this subfamily of proteins and accordingly went about probing their roles. The mutational analysis clearly implicates that T330 is important for the binding of PLP. The enzyme loses the ability to bind to PLP even if this residue is mutated conservatively to T330S or T330A. E243 has been implicated in specificity. In human Ornithine aminotransferase, the Glu-to-Ala mutation made it 10^6 times more specific for substrate Glu compared to its natural substrate ornithine [23]. In the case of MtLAT the analogous E243A mutant retained activity, but interestingly the C5 substrate KGA adopts a different conformation in the crystal structure with the mutant compared to the native enzyme. Changes to the substrate specificity, if any, remain to be tested in this case. Examination of the crystal structure of the E243A mutant and superposition of the substrate Glu onto KGA is instructive. Although KGA adopts a different conformation, the superposition suggests that the O5 atom of KGA has a similar spatial disposition in its complexes with the mutant and the native enzyme. Accordingly the superposed α-carboxylate of Glu is within striking distance of the N4 atom of PMP to initiate the second half reaction. This analysis agrees with the observed activity of the E243A mutant. N328 interacts with the substrates and probably helps stabilize it. Clearly this important role is lost in the N328A mutant. The enzyme, however, retains the ability to bind to the co-factor as seen in the crystal structures.

The inhibitor was originally identified through virtual screening approaches [11]. It mimics the binding of C5 substrates and adopts two different binding modes. Also, the phenacyl group of the inhibitor displaces two conserved structural water molecules. Our analysis of the active site water molecules was based on this observation and is aimed at improving the affinity of the next generation of inhibitors. The analysis suggests that a strategy of displacing and replacing the network of interactions involving the conserved waters, especially W4–W9 Fig. 4, could be advantageous in improving inhibitor efficacy. Ongoing synthesis experiments are based on these results.

Conflict of interest

None.

Acknowledgments

We thank Dr. Amit Sharma, ICGEB, New Delhi, for permitting collection of a data set at ICGEB, New Delhi. S.M.T. acknowledges University *Grants Commission*, India, for a Senior Research Fellowship. *Council of Scientific and Industrial Research (CSIR)*, India funded this work through grants BSC0104 (Splendid) and BSC0121 (Genesis) respectively. AA is a CSIR senior research fellow. This manuscript bears the CDRI communication number 8997.

Transparency document

Transparency document related to this article can be found online at http://dx.doi.org/10.1016/j.bbrc.2015.05.055.

References

[1] T. Fujii, T. Narita, H. Agematu, et al., Characterization of L-lysine ε -aminotransferase and its structural gene from flavobacteriumlutescens IFO3084, J. Biochem. 128 (2000) 391–397.
[2] M.B. Tobin, S. Kovacevic, K. Madduri, et al., Localization of the lysine ε-aminotransferase (lat) and δ-(L-α-aminoadipyl)-L-cysteinyl-D-valinesynthetase(pcbAB) genes from *Streptomyces clavuligerus* and production of lysine ε-aminotransferase activity in *Escherichia coli*, J. Bacteriol. 173 (1991) 6223–6229.
[3] D. Schiroli, A. Peracchi, A subfamily of PLP-dependent enzymes specialized in handling terminal amines, Biochim. Biophys. Acta (2015), http://dx.doi.org/10.1016/j.bbapap.2015.02.023.
[4] S.M. Tripathi, R. Ramachandran, Direct evidence for a glutamate switch necessary for substrate recognition: crystal structures of lysine ε-aminotransferase (Rv3290c) from *Mycobacterium tuberculosis* H37Rv, J. Mol. Biol. 362 (2006) 877–886.

[5] S.M. Tripathi, R. Ramachandran, Overexpression, purification and crystallization of lysine ε-aminotransferase (Rv3290c) from *Mycobacterium tuberculosis* H37Rv, Actacrystallograph. Sect. F Struct. Biol. Cryst. Commun. 62 (2006) 572–575.
[6] H. Hayashi, Pyridoxal enzymes: mechanistic diversity and uniformity, J. Biochem. 118 (1995) 463–473.
[7] B.W. Shen, M. Henning, E. Hohenester, et al., Crystal structure of human recombinant ornithine aminotransferase, J. Mol. Biol. 277 (1998) 81–102.
[8] P. Storici, D.D. Biase, F. Bossa, et al., Structures of γ-aminobutyric acid (GABA) aminotransferase, a pyridoxal 5′-phosphate, and [2Fe-2S] cluster containing enzymes, complexed with γ-ethynyl-GABA and with the antiepilepsy drug vigabatrin, J. Biol. Chem. 279 (2004) 363–373.
[9] TB-Structural-Genomics Consortium, PLOS Comp. Biol. 2 (2006) 539–550.
[10] D.J. Murphy, J.R. Brown, Identification of gene targets against dormant phase *Mycobacterium tuberculosis* infections, BMC Infect. Dis. 7 (2007) 84, http://dx.doi.org/10.1186/1471-2334-7-84.
[11] D. Dube, S.M. Tripathi, R. Ramachandran, Identification of in vitroinhibitors of *Mycobacterium tuberculosis* lysine ε -aminotransferase by pharmacophore mapping and three-dimensional flexible searches, Med. Chem. Res. 17 (2008) 182–188.
[12] K. Soda, H. Misono, T. Yamamoto, L-lysine α-ketoglutarate aminotransferase: I. Identification of product, Δ 1-piperidine-6-carboxylic acid, Biochemistry 7 (1968) 4102–4109.
[13] B. Bhaskar, V. Prakash, H.S. Savithri, et al., Interactions of l-serine at the active site of serine hydroxymethyltransferases: induction of thermal stability, Biochim Biophys Acta 1209 (1994) 40–50.
[14] A.G.W. Leslie, Joint CCP4 + ESF-eamcb Newsletter on Protein Crystallography, No. 26, 1992.
[15] P.R. Evans, Proceedings of the CCP4 Study Weekend. Data Collection and Processing, Daresbory Laboratory, Warrigton, 1993, pp. 114–1222.
[16] Collaborative computational project, N, Acta Crystallogr. D 50 (1994) 760–763.
[17] T.A. Jones, A graphic model building and refinement system for macromolecules, J. Appl. Crystallogr. 11 (1989) 268–272.
[18] P. Emsley, K. Cowtan, Acta Crystallogr. D 60 (2004) 2126–2132.
[19] R. Ravishankar, K. Suguna, A. Surolia, et al., Structures of the complexes of peanut lectin with methyl–galactose and N-acetyllactosamine and a comparative study of carbohydrate binding in Gal/GalNAc-specific legume lectins, Acta Crystallogr. D 55 (1999) 1375–1382.
[20] R. Frederick, C. Charlier, S. Robert, et al., Investigation of mechanism-based thrombin inhibitors: implications of a highly conserved water molecule for the binding of coumarins within the S pocket, Bioorg. Med. Chem. Lett. 16 (2006) 2017–2021.
[21] S.T. Cole, R. Brosch, J. Parkhill, et al., Deciphering the biology of *Mycobacterium tuberculosis* from the complete genome sequence, Nature 393 (1998) 537–544.
[22] J.C. Betts, P.T. Luckey, L. Robb, et al., Evaluation of a nutrient starvation model of *Mycobacterium tuberculosis* persistence by gene and protein expression profiling, Mol. Microbiol. 43 (2002) 717–731.
[23] M. Markova, C. Peneff, M.J.E. Hewlins, et al., Determinants of substrate specificity in ω-aminotransferases, J. Biol. Chem. 280 (2005) 36409–36416.